A Prospective Longitudinal Study of Retinal Structure and Function in Achromatopsia

Jonathan Aboshiha,[1,2] Adam M. Dubis,[1,2] Jill Cowing,[1] Rachel T. A. Fahy,[1] Venki Sundaram,[2] James W. Bainbridge,[1,2] Robin R. Ali,[1] Alfredo Dubra,[3,4] Marko Nardini,[5] Andrew R. Webster,[1,2] Anthony T. Moore,[1,2] Gary Rubin,[1] Joseph Carroll,[3,4,6] and Michel Michaelides[1,2]

[1]UCL Institute of Ophthalmology, University College London, London, United Kingdom
[2]Moorfields Eye Hospital, London, United Kingdom
[3]Department of Ophthalmology, Medical College of Wisconsin, Milwaukee, Wisconsin, United States
[4]Department of Biophysics, Medical College of Wisconsin, Milwaukee, Wisconsin, United States
[5]Department of Psychology, Durham University, Durham, United Kingdom
[6]Department of Cell Biology, Neurobiology, and Anatomy, Medical College of Wisconsin, Milwaukee, Wisconsin, United States

Correspondence: Michel Michaelides, UCL Institute of Ophthalmology, 11-43 Bath Street, London, EC1V 9EL, UK;
michel.michaelides@ucl.ac.uk.

JC and MM are joint senior authors.

Submitted: June 2, 2014
Accepted: July 27, 2014

Citation: Aboshiha J, Dubis AM, Cowing J, et al. A prospective longitudinal study of retinal structure and function in achromatopsia. *Invest Ophthalmol Vis Sci*. 2014;55:XXXX–XXXX. DOI:10.1167/iovs.14-14937

Purpose. To longitudinally characterize retinal structure and function in achromatopsia (ACHM) in preparation for clinical gene therapy trials.

Methods. Thirty-eight molecularly confirmed ACHM subjects underwent serial assessments, including spectral domain optical coherence tomography (SD-OCT), microperimetry, and fundus autofluorescence (FAF). Foveal structure on SD-OCT was graded and compared for evidence of progression, along with serial measurements of foveal total retinal thickness (FTRT) and outer nuclear layer (ONL) thickness. Fundus autofluorescence patterns were characterized and compared over time.

Results. Mean follow-up was 19.5 months (age range at baseline, 6–52 years). Only 2 (5%) of 37 subjects demonstrated change in serial foveal SD-OCT scans. There was no statistically significant change over time in FTRT ($P = 0.83$), ONL thickness ($P = 0.27$), hyporeflective zone diameter ($P = 0.42$), visual acuity ($P = 0.89$), contrast sensitivity ($P = 0.22$), mean retinal sensitivity ($P = 0.84$), and fixation stability ($P = 0.58$). Three distinct FAF patterns were observed ($n = 30$): central increased FAF ($n = 4$), normal FAF ($n = 11$), and well-demarcated reduced FAF ($n = 15$); with the latter group displaying a slow increase in the area of reduced FAF of 0.03 mm^2 over 19.3 months ($P = 0.002$).

Conclusions. Previously published cross-sectional studies have described conflicting findings with respect to the age-dependency of progression. This study, which constitutes the largest and longest prospective longitudinal study of ACHM to date, suggests that although ACHM may be progressive, any such progression is slow and subtle in most patients, and does not correlate with age or genotype. We also describe the first serial assessment of FAF, which is highly variable between individuals, even of similar age and genotype.

Keywords: achromatopsia, gene therapy, optical coherence tomography, retinal dystrophy, retinal degeneration

Achromatopsia (ACHM) is an autosomal recessive cone dysfunction syndrome affecting approximately 1 in 30,000 people, and characterized by the presentation in infancy of pendular nystagmus, poor visual acuity, and photophobia.[1] Electroretinography (ERG) demonstrates absent cone responses and normal or near-normal rod responses,[2,3] with psychophysical testing revealing normal rod function but absent or severely reduced cone function.[4] To date, five genes have been found to be associated with ACHM, all encoding components of the cone-specific phototransduction cascade. The two most common of these are *CNGA3*[5] and *CNGB3*,[6] encoding the α- and β-subunits of the cGMP-gated cation channel respectively, and together account for approximately 70% of cases.[7] Disease-causing sequence variants also have been identified in *GNAT2*,[8] *PDE6C*,[9] and *PDE6H*,[10] each responsible for fewer than 2% of cases.[8–10]

Several studies recently demonstrated the effectiveness of using a gene-replacement approach to restore cone function in dog and mouse models of ACHM,[11–14] and the neuroprotective protein ciliary neurotrophic factor also has been shown to induce a transient restoration of cone function and visually directed behavior in the *CNGB3* dog model.[15] Given these promising results, there are plans to begin human clinical trials in the near future. This makes the accurate measurement and stratification of retinal structure and function in ACHM critical, both in terms of patient selection and subsequent assessment of treatment response.

Achromatopsia has been classically described as stationary[1,2,7]; however, several recent studies have suggested it is a progressive condition. Thiadens et al.[16] examined 40 ACHM patients using spectral-domain optical coherence tomography (SD-OCT), and reported that increased cone cell "decay" and retinal thinning was correlated with age, and began in early

childhood. They reported that cone loss, as assessed on SD-OCT, occurred in 42% (8 of 19) of the achromats aged younger than 30 years, whereas this finding was observed in 95% (20 of 21) of patients older than 30 years. Thomas et al.[17] also noted in their study ($n = 13$) that the existence of a hyporeflective zone (HRZ) and outer nuclear layer (ONL) thinning were both age dependent. In contrast to these studies, Genead et al[18] carried out a variety of investigations to assess macular structure, including SD-OCT ($n = 12$), and found that there was significant structural variability even within individuals of the same genotype and age. They also found adaptive optics scanning light ophthalmoscopy (AOSLO) evidence of residual cone inner segment structure in all but one of the nine patients assessed, including the oldest patient (55 years), suggesting that progressive and complete loss of cones in ACHM may not be inevitable, and was not obviously age-dependent. Sundaram et al.[19] examined 40 ACHM patients aged 6 to 52 years, and found no correlation between age and visual acuity, total foveal thickness, foveal ONL thickness, or inner segment ellipsoid (ISe) intensity and cone loss on SD-OCT.

All of these studies are inherently limited by their cross-sectional nature, and the debate surrounding whether there is, or is not, age-dependent cone loss highlights the need for prospective longitudinal studies of large cohorts of molecularly proven patients. Thomas et al.[20] followed eight patients longitudinally, over a mean period of 16 months. They reported that the five younger patients (aged <10 years) demonstrated progressive disturbance at the foveal photoreceptor inner segment/outer segment junction on OCT; but the three older patients (aged >40 years) did not. Due to the small number of patients, they were not able to perform statistical comparisons between the two visits.

A further means of assessing macular integrity is through the use of fundus autofluorescence (FAF),[21] which can act as a surrogate measure of photoreceptor health.[22] There are limited data concerning FAF patterns in ACHM. Michaelides et al.[23] reported that the FAF appearance was normal in five affected members of a *GNAT2* family. In a recent study of 10 achromats, Fahim et al.[24] suggested an age-dependent change in FAF, with younger patients exhibiting increased foveal autofluorescence (AF), whereas older patients had reduced AF with discrete borders corresponding to outer retinal defects on SD-OCT. Greenberg et al.[25] also observed FAF abnormalities, including increased and/or decreased AF ($n = 17$). However, again these were cross-sectional studies of relatively small size, with no longitudinal FAF data in ACHM published to date. There is a need to assess whether FAF signals in ACHM change over time, which might aid assessment of any progression, genotype characterization, and potentially serve as a marker for response to future interventions.

Here we performed serial assessments of visual acuity, contrast sensitivity, microperimetry (MP), SD-OCT, and FAF, in the largest longitudinal study of molecularly proven patients to date, with the goal of providing statistically supported conclusions regarding the relative frequency and rate of any observed progression.

Methods

Subjects

Forty subjects who had been characterized both phenotypically (including electrophysiologically) and genotypically in a previously published cross-sectional study[19] were prospectively asked to return for follow-up assessment at an interval of between 12 and 24 months after baseline assessment. The study protocol adhered to the Tenets of the Declaration of Helsinki, and was approved by the Moorfields Eye Hospital Ethics Committee. Informed consent was obtained from all subjects before entering the study.

Clinical Assessments

A detailed follow-up assessment was undertaken that included best-corrected visual acuity (BCVA) using an Early Treatment Diabetic Retinopathy Study chart, contrast sensitivity assessment using the Pelli-Robson chart at 1 m, MP, SD-OCT, and FAF. All assessments were prospectively standardized to be undertaken in the same conditions in the follow-up assessment as at baseline assessment.

Spectral-Domain OCT

After pupillary dilation with tropicamide 1% and phenylephrine 2.5% eye drops, line and volume scans were obtained using a Spectralis SD-OCT on both eyes (Heidelberg Engineering, Heidelberg, Germany) using the same protocol as used in the baseline cross-sectional study.[19] Briefly, the volume acquisition protocol consisted of 49 B-scans (124 μm between scans; 20° × 20°), with Automatic Real Time eye tracking used whenever possible. During follow-up assessment, the Spectralis SD-OCT was engaged in its follow-up mode, to ensure that the same scanning location was identified at both time points. This is achieved by setting the baseline scan as the reference scan, and the inbuilt software then ensures that the SD-OCT laser is directed to the same retinal location during subsequent image acquisition.[26] The lateral scale of each image was estimated using the axial length of the corresponding eye, obtained from the Zeiss IOL Master (Carl Zeiss Meditec, Jena, Germany).

Qualitative assessment of foveal morphology was undertaken by grading foveal structure on SD-OCT images into one of five categories: (1) continuous ISe, (2) ISe disruption, (3) ISe absence, (4) presence of an HRZ, or (5) outer retinal atrophy, including loss of RPE (Fig. 1). The presence or absence of foveal hypoplasia was also noted, and was defined as the persistence of one or more inner retinal layer (outer plexiform layer, inner nuclear layer, inner plexiform layer, or ganglion cell layer) through the fovea. Consensus grading was established by three independent examiners (JA, JCarroll, and MM). Measurements of foveal total retinal thickness (FTRT) (internal limiting membrane to RPE distance), foveal ONL thickness, and, where relevant, HRZ diameter, were made by a single observer (JA) at baseline and follow-up scans, using the digital calipers built into the software (Heidelberg Eye Explorer; Heidelberg Engineering), and a 1-pixel:1-μm display with maximal magnification. In cases of foveal hypoplasia, the distance between the posterior outer plexiform layer and the external limiting membrane was taken as the ONL thickness. The mean of three measurements was used. Due to the optimum image resolution, imaging speed and follow-up acquisition mode and eye-tracking used in the Spectralis SD-OCT, retinal thickness measurements using this device have been shown to be highly reproducible,[26] and this method of assessing foveal thickness in the assessment of macular pathology has been used elsewhere.[27,28]

Fundus Autofluorescence

Fundus autofluorescence was performed at baseline and follow-up assessments using the AF mode built in to the Spectralis confocal scanning laser ophthalmoscope (Heidelberg Engineering). All images were acquired after mydriasis as described above, and after the SD-OCT image acquisition protocol was complete, due to the relatively intense lights used

Investigative Ophthalmology & Visual Science

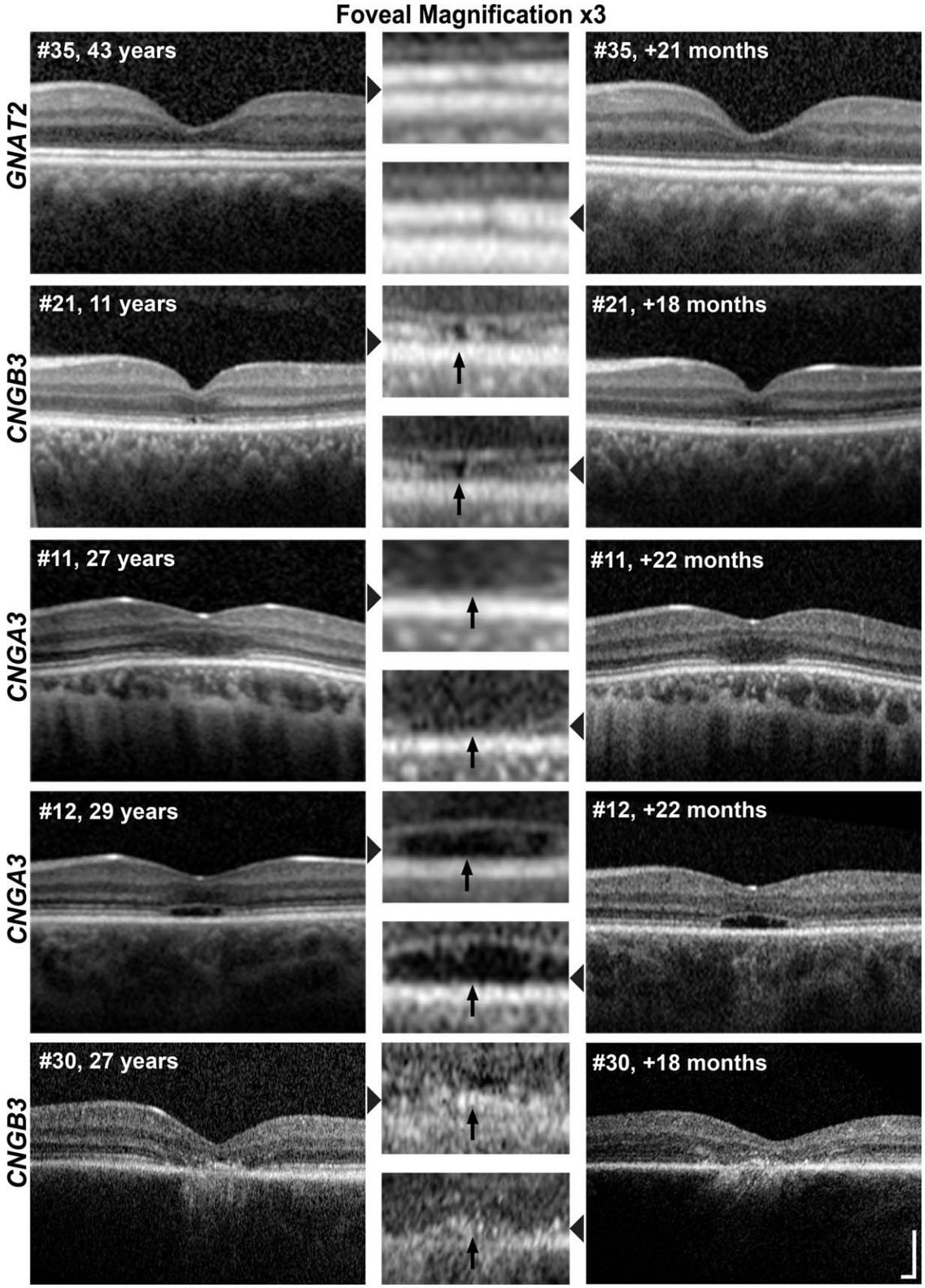

Figure 1. Longitudinal SD-OCT scans in achromatopsia. *Left*: Baseline scans indicating genotype, patient number, and age at initial scan. *Right*: Follow-up scans indicating patient number and interval between baseline and follow-up scans in months. *Center*: Foveal magnification (×3) of corresponding scan (*gray arrows*). Shown are the left eyes of a typical subject from each of the five SD-OCT categories, all of whom demonstrated no change in SD-OCT structure over the study period (from the top row down: patient 35 with a continuous ISe band at both time points; patient 21 with a disrupted ISe layer at both time points; patient 11 with an absent ISe layer at both time points; patient 12 with an HRZ at both time points; and patient 30 with outer retinal atrophy at both time points). Nonmagnified images represent 4500 μm horizontally and 1000 μm vertically; image scaling has been corrected for axial length. *Scale bar*: 200 μm.

Investigative Ophthalmology & Visual Science

during FAF acquisition and the photophobic nature of achromats. Images were acquired using a 30° field, with an optically pumped solid-state laser producing an excitation wavelength of 488 nm. The induced AF was detected through a barrier filter of 500 nm, and acquired after focusing the retinal image using the 820-nm infrared mode and sensitivity adjustment at 488 nm.

In the case of patients who had areas of abnormally reduced AF signal, measurements of this area were performed by describing this region with a mouse-driven cursor, and recording the area given by the in-built image analysis software (Heidelberg Eye Explorer; Heidelberg Engineering); this method has been used in the assessment of progressive macular disease elsewhere.[29,30] All FAF measurements were made by a single observer (JA), and for each FAF image, the mean of three area measurements was calculated and used for further analysis.

Microperimetry

Microperimetry (MP) was performed in all subjects on both eyes, and after pupillary dilation, in a darkened room using the MP1 microperimeter (Nidek Technologies, Padova, Italy) in follow-up mode, and otherwise using the same testing conditions as at baseline assessment.[19] Two tests were undertaken on each eye, using a customized test grid of 44 retinal locations situated within an 8° radius to cover the macular and paramacular region, and over which the mean retinal sensitivity was recorded. During each test, the non-tested contralateral eye was occluded.

Background illuminance was set within the mesopic range (1.27 cd/m^2), and patients maintained fixation by looking at a 2° target. A variable intensity Goldmann size III (4 mm^2) stimulus of 200-ms duration was used as the testing stimulus. A 4-2 testing strategy was used, with the intensity of the stimulus reduced in 4-dB steps until the patient no longer detected it. The stimulus intensity then increased in 2-dB steps until detected once again. Projection of the stimulus into the blind spot at 30-second intervals tested for false-positive errors. Fixation stability was assessed using the bivariate contour ellipse area (BCEA) analysis, which represents an area in degrees where 68% (i.e., 1 SD) of fixation points are located[31]; this value is reported by the Nidek software. An active eye-tracking system ensured accurate stimulus projection in relation to retinal landmarks to correct for fixation errors.

Data Analysis Methods

Histogram plots were used to verify the normality of data before the use of any parametric tests. Statistical analyses were performed using GraphPad Prism, version 5 (GraphPad Software, Inc., La Jolla, CA, USA). As the left eye had been selected for further analysis in the original cross-sectional study (which had found no significant difference in measured parameters between eyes),[19] this eye also underwent detailed further analysis in the follow-up study. Patient identification numbers were kept the same as in the cross-sectional study for ease of reference. Variability indicators (±) represent 1 SD in normally distributed metrics.

Results

Thirty-eight (95%) of the 40 patients who were assessed at baseline were able to attend for follow-up assessment within the 12- to 24-month study recall window. Two female patients were unable to return; one due to the onset of unrelated long-term illness (patient 25) and the other due to pregnancy (patient 32). Of the 38 patients who were followed up, 20 were male (53%) and 18 were female (47%). The mean age of the follow-up cohort was 25 years at baseline (±12.5; range, 6–52 years), with a mean follow-up interval of 19.5 months (±2.8 months; range, 13–24 months). The Table summarizes the clinical findings, and includes age at baseline, interval of follow-up period, genotype, and functional and structural parameters over time.

Best Corrected Visual Acuity and Contrast Sensitivity

The mean BCVA at baseline was 0.92 logMAR (±0.13; range, 0.74–1.32 logMAR), and was not significantly different from the mean BCVA at follow-up, which also measured 0.92 logMAR (±0.11; range, 0.74–1.28 logMAR) (paired *t*-test; $P = 0.89$). The mean of the logarithm of the contrast sensitivity (logCS) at baseline of 1.16 logCS (±0.23; range, 0.5–1.55 logCS) was also not significantly different from that measured at follow-up of 1.21 logCS (±0.32; range, 0.25–1.65 logCS) (paired *t*-test; $P = 0.22$); where higher logCS values indicate better contrast sensitivity.

Spectral-Domain OCT

In 37 of the 38 patients who underwent serial SD-OCT, foveal scans were acquired at baseline and follow-up that were comparable across time points. In one patient (patient 1) foveal follow-up SD-OCT images could not be obtained due to poor fixation, and this patient was excluded from further SD-OCT analysis. Two (5%) of these 37 patients demonstrated progression on SD-OCT between time points: patient 2 (10 years old at first visit) progressed from category 1 (continuous ISe layer) at baseline to category 2 (ISe disruption) over a 20-month period, and patient 31 (33 years old at first visit) progressed from category 2 (ISe disruption) to category 4 (HRZ) over the same number of months (Fig. 2). However, these observed changes were subtle in patient 2, and the SD-OCT findings of patient 31 at baseline, with the high reflectivity foveal lesion, are not typically seen in ACHM. No other patients showed evidence of progression, either in terms of transition to another SD-OCT category or progression within a category (Fig. 1).

The right eye SD-OCT images of all patients were also graded at baseline and follow-up assessment, given that in the cross-sectional study no parameter measured demonstrated any significant difference between eyes,[19] and so presumably any change over time observed in both eyes would more likely represent real disease progression. Both patients with SD-OCT evidence of progression in the left eye showed similar deterioration in the right eye (Fig. 2), whereas the remaining patients had the same SD-OCT appearance in the right eye at baseline and follow-up, as was the case for their left eyes. The changes in patient 2 were again subtle in the right eye, but that the SD-OCT changes were mirrored in both eyes in both patients 2 and 31 would lend support to the view that the morphological change detected in these two patients was real.

The remaining 35 patients (95%) showed no evidence of deterioration in SD-OCT appearance on qualitative assessment (Fig. 1). No patients had a change in the presence or absence of foveal hypoplasia between baseline and follow-up assessment.

Foveal Total Retinal Thickness, ONL Thickness, and HRZ Diameter

Foveal total retinal thickness was measured in all 37 patients who had serial foveal SD-OCT assessments. There was no

Table. Summary of Clinical Findings

Patient No.	Age at Baseline, y	f/u Interval, mo	Genotype	BCVA, logMAR		Contrast Sensitivity, logCS		MP Mean Sensitivity, dB		MP Mean BCEA, (°)		SD-OCT Category*		Change in FTRT Between Assessments, µm	Change in ONL Thickness Between Assessments, µm	Central FAF Pattern at Both Assessments
				b	f/u	b	f/u	b	f/u	b	f/u	b	f/u			
1	7	21	*CNGA3*	0.94	0.86	1.30	1.40	14.90	16.20	44.04	36.70	3	N/A	N/A	N/A	N/A
2	10	20	*CNGA3*	0.80	0.82	1.25	1.55	19.67	19.75	15.82	8.05	1	2	+3	−10	Normal
3	11	16	*CNGA3*	1.08	1.04	0.90	1.10	14.90	14.50	40.70	61.80	1	1	+2	+2	N/A
4	11	17	*CNGA3*	0.94	1.00	1.05	1.30	17.60	19.50	14.75	17.90	2	2	+3	−1	Increased
5	17	16	*CNGA3*	0.80	0.86	1.20	1.35	18.35	18.55	6.00	7.35	3	3	−9	−1	Reduced
6	19	21	*CNGA3*	0.80	0.92	0.65	0.50	17.57	14.85	3.51	3.45	2	2	+2	0	Reduced
7	22	16	*CNGA3*	1.16	1.06	1.05	1.00	15.55	15.35	3.91	5.90	2	2	+3	+3	Normal
8	22	22	*CNGA3*	0.92	0.92	1.35	1.50	17.60	19.15	5.48	4.45	4	4	−3	−7	Normal
9	24	22	*CNGA3*	0.90	0.86	1.20	1.35	19.30	18.55	16.80	8.35	2	2	+2	+2	Normal
10	25	22	*CNGA3*	0.84	0.84	1.35	1.45	3.10	5.80	3.61	24.40	5	5	+4	N/A	Reduced
11	27	22	*CNGA3*	0.84	0.76	1.05	1.55	17.67	17.80	7.92	4.25	3	3	−7	−6	Reduced
12	29	22	*CNGA3*	0.74	0.90	1.20	1.25	13.55	15.20	37.43	7.60	4	4	+3	+2	Reduced
13	29	21	*CNGA3*	0.90	0.92	1.55	1.55	19.20	18.25	7.74	5.00	2	2	−8	−3	Increased
14	31	22	*CNGA3*	0.90	0.92	1.45	1.25	17.95	17.00	2.00	8.90	4	4	−2	+2	Normal
15	31	21	*CNGA3*	0.84	0.84	1.25	1.50	17.63	15.90	17.88	36.10	2	2	0	−4	N/A
16	34	21	*CNGA3*	0.90	0.82	1.20	1.05	13.80	14.90	10.20	14.40	2	2	−1	+3	Normal
17	35	21	*CNGA3*	0.96	0.96	0.90	1.00	14.17	15.90	13.15	7.60	2	2	−4	+2	Normal
18	49	17	*CNGA3*	0.80	0.74	1.30	1.30	17.15	18.25	2.23	2.95	4	4	+1	+2	Reduced
19	6	17	*CNGB3*	1.08	1.08	1.20	1.10	14.75	16.50	65.00	28.30	1	1	+2	−2	N/A
20	11	15	*CNGB3*	0.82	0.86	1.05	1.15	19.65	19.20	19.13	28.20	4	4	0	−1	Reduced
21	11	18	*CNGB3*	0.90	0.88	1.35	1.20	18.35	19.00	5.23	3.30	2	2	0	+3	Increased
22	13	21	*CNGB3*	0.90	1.00	1.00	1.10	18.93	19.25	8.62	8.80	3	3	−3	+3	Normal
23	12	16	*CNGB3*	0.76	0.80	1.30	1.35	19.80	19.05	5.97	3.95	2	2	+3	−4	Normal
24	13	18	*CNGB3*	0.90	0.82	1.30	1.50	19.27	19.95	6.54	6.00	1	1	−8	+1	Increased
26	18	24	*CNGB3*	0.74	0.76	1.25	1.40	18.40	17.80	3.70	4.10	4	4	+3	+2	Reduced
27	19	17	*CNGB3*	0.86	0.88	1.35	1.35	18.50	17.10	3.75	2.60	4	4	+3	−3	N/A
28	23	13	*CNGB3*	0.76	0.80	1.25	1.55	18.35	17.75	6.32	6.40	5	5	+4	N/A	Reduced
29	24	20	*CNGB3*	0.90	0.92	1.45	1.65	15.00	14.80	3.27	3.60	1	1	−2	−2	N/A
30	27	18	*CNGB3*	1.20	1.04	1.15	1.00	14.63	15.75	38.02	44.95	5	5	+2	N/A	Reduced
31	33	20	*CNGB3*	0.96	0.84	0.90	1.20	16.65	18.00	15.12	11.90	2	4	+3	+3	Reduced
33	47	13	*CNGB3*	0.96	1.00	1.10	1.15	19.35	17.00	7.30	5.00	4	4	+3	−1	Reduced
34	29	24	*GNAT2*	0.88	0.94	1.20	0.25	14.30	14.80	2.09	1.70	4	4	−2	0	Reduced
35	43	21	*GNAT2*	1.10	1.10	0.70	0.75	14.83	12.30	16.56	15.70	1	1	−4	−1	Reduced
36	49	21	*GNAT2*	0.94	1.04	1.05	0.75	13.43	13.20	10.31	11.70	1	1	−1	−1	Normal
37	52	21	*GNAT2*	1.00	1.00	0.50	0.65	14.80	14.30	20.90	18.95	1	1	+1	0	Normal
38	43	21	*PDE6C*	1.32	1.28	1.05	0.80	7.77	7.70	17.15	11.85	3	3	+2	+1	Reduced
39	19	21	?	0.96	0.92	1.45	1.55	19.57	18.80	9.54	20.10	3	3	+2	−5	N/A
40	23	21	?	0.86	0.74	1.20	1.35	19.83	19.75	16.14	10.85	3	3	0	0	N/A

Patient number as in Sundaram et al.[19] b, baseline; f/u, follow-up; BCVA, best corrected visual acuity; OD, right eye; OS, left eye; LogMAR, logarithm of the minimum angle of resolution; LogCS, logarithm of contrast sensitivity; MP, microperimetry; dB, decibels; BCEA, bivariate contour ellipse area; SD-OCT, spectral-domain optical coherence tomography; ISe, inner segment ellipsoid; RPE, retinal pigment epithelium; N/A, not assessable; FTRT, foveal total retinal thickness; ONL, outer nuclear layer; +, increase in metric over time between assessments; −, reduction over time; FAF, fundus autofluorescence; ?, no disease-causing variant identified in *CNGA3*, *CNGB3*, *GNAT2*, *PDE6C*, or *PDE6H*.

*SD-OCT category: 1, continuous ISe; 2, ISe disruption; 3, ISe absence; 4, HRZ present; 5, outer retinal atrophy.

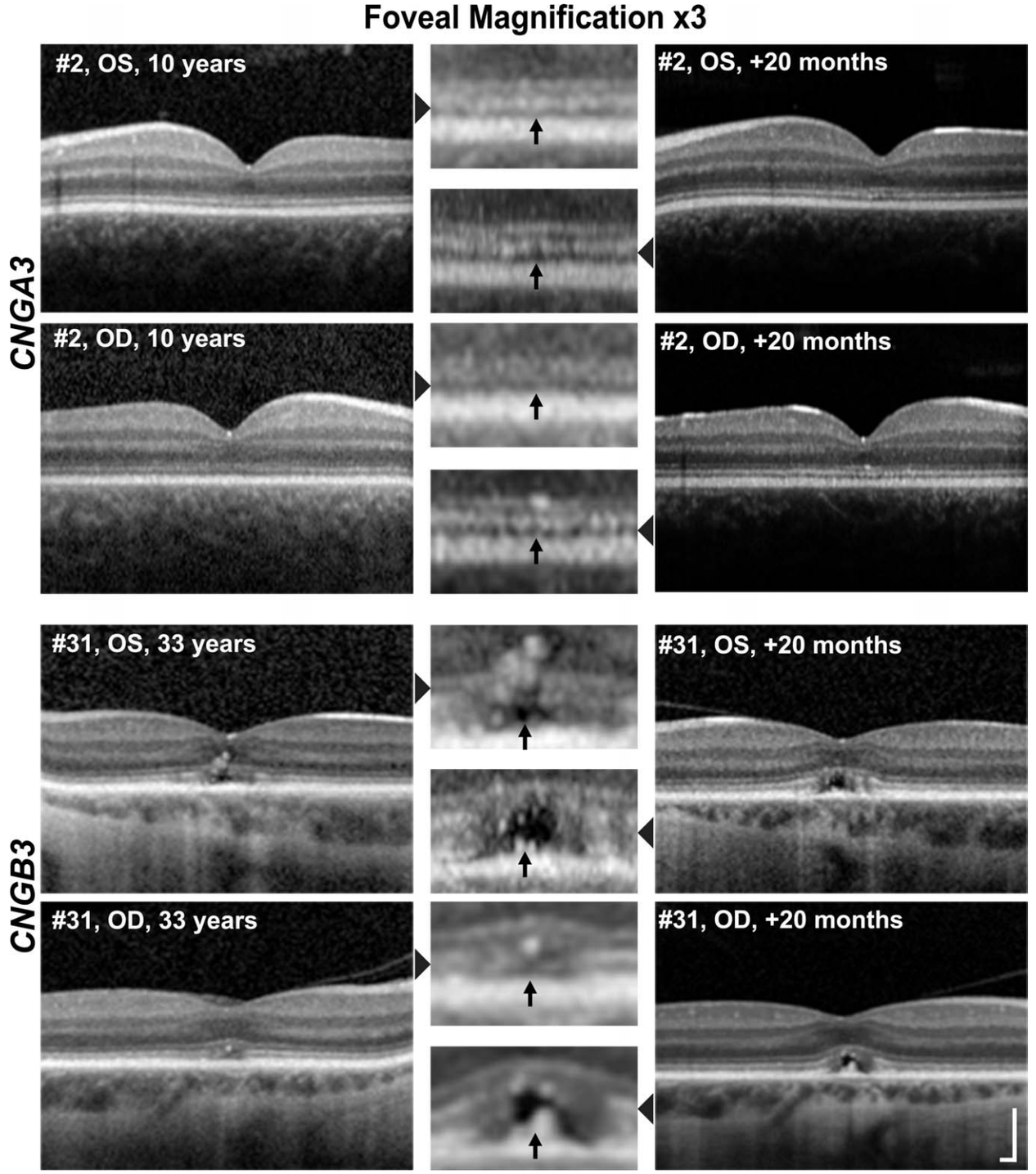

Figure 2. The left and right eye scans of the two achromatopsia subjects who demonstrated a change in SD-OCT appearance over the time course of the study. Layout is as in Figure 1. *Top two rows*: Patient 2 showed a continuous ISe layer at the fovea at initial scan in both the OS and OD eyes, and subsequently a disrupted ISe layer in both eyes at follow-up scan 20 months later (*black arrows*). *Bottom two rows*: Patient 31 showed a disrupted ISe layer at initial scan in both eyes and an HRZ 20 months later (*black arrows*). Nonmagnified images represent 4500 μm horizontally and 1000 μm vertically; image scaling has been corrected for axial length. *Scale bar*: 200 μm.

statistically significant change between visits (i.e., follow-up thickness minus baseline thickness; negative numbers indicating thinning over time) in FTRT in the cohort, with mean change of −0.1 μm (95% confidence interval (CI) −1.3 to +1.1 μm; range, −9 to +4 μm) (paired *t*-test; $P = 0.83$) (Table).

Three (8%) of the 37 patients who underwent serial foveal SD-OCT scanning (patients 10, 28, and 30) did not have a structurally-distinct ONL layer that could be accurately measured, and so were excluded from the ONL thickness analysis. The mean ONL thickness change in the remaining 34

Investigative Ophthalmology & Visual Science

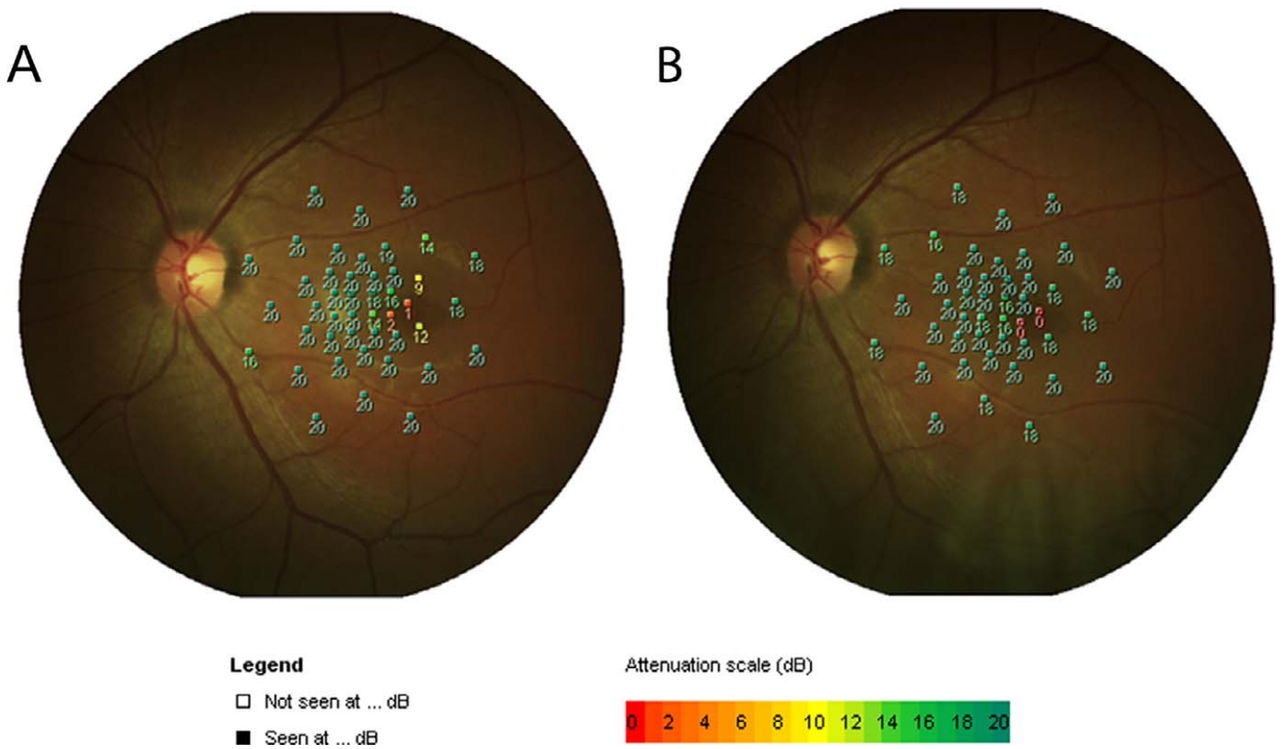

FIGURE 3. The microperimetry findings in patient 5, who developed a scotoma during this study. (**A**) Microperimetry findings at baseline. Numbers indicate retinal sensitivity (dB) at that location. (**B**) Microperimetry findings 16 months later indicate an absolute scotoma at two locations.

patients of −0.6 μm (95% CI −1.7 to +0.5 μm; range, −10 to +3 μm) was not statistically significant between assessments (paired *t*-test; $P = 0.27$) (Table). Only one patient had ONL thinning of 10 μm or more (patient 2 with 10 μm), which is in keeping with the qualitative deterioration of outer retinal structure on SD-OCT observed in this patient. In the nine patients who had an HRZ at both time point assessments, there was no statistically significant change in the diameter of the HRZ over a mean follow-up time of 19.6 months in this group (paired *t*-test; $P = 0.42$).

Microperimetry

All 38 patients underwent follow-up MP testing on two or more occasions, and the mean of these tests was used for subsequent analysis. The mean retinal sensitivity of this cohort at baseline was 16.6 dB (±3.4; range, 3.1–19.9 dB), and was not significantly different from that measured at follow-up (16.5 dB ±3.07; range, 5.8–16.5 dB) (paired *t*-test; $P = 0.84$) (Table). The fixation stability measured at baseline (median = 9.1°; range, 1.7–65°) was also not significantly different from that at follow-up (median = 8.2°; range, 1.7–61.8°) (Wilcoxon matched-pairs signed rank test; $P = 0.58$) (Table). At baseline assessment, six subjects had a scotoma (defined as 0 dB sensitivity in ≥1 retinal location). Follow-up MP assessment also showed that the same six patients had scotomas. In addition, one further patient (patient 5, 17 years old at baseline assessment) developed a scotoma that was not apparent on initial testing, and was evident in both follow-up MP tests 16 months later (Fig. 3). However, the change in point sensitivity is small and would fall within intertest variability limits, as can be seen in the variation in sensitivities in the points around those that developed an absolute scotoma.

Fundus Autofluorescence

In 30 (84%) of the 38 patients, baseline and follow-up FAF images were of sufficient quality to enable accurate classification and, where necessary, measurement of the area of reduced FAF signal. Several patients experienced discomfort with the bright light needed to acquire FAF images, and given their extreme photophobia, this contributed to relatively lower patient concordance and successful acquisition compared with other serial assessment modalities. We observed three FAF patterns at baseline ($n = 30$): (1) a normal FAF pattern, seen in 11 patients (37%); (2) an abnormal central increase in FAF, seen in 4 patients (13%); and (3) a discretely bordered abnormal central reduction in FAF, seen in 15 patients (50%) (Fig. 4). No change in the type of FAF pattern was observed between baseline and follow-up assessments, or between eyes, in any of the patients.

Given that the reduced FAF pattern had well-demarcated borders amenable to quantification, the area of reduced FAF was measured at baseline and follow-up in the 15 patients with this FAF phenotype. There was a small but statistically significant increase in median area of reduced FAF between assessments (Wilcoxon matched-pairs test; $P = 0.002$), with the median change being +0.03 mm² (interquartile range, +0.01 to +0.13 mm²; range, 0 to +0.28 mm²), where positive numbers indicate an increase in the area of reduced FAF signal over the mean follow-up time in this subgroup of 19.3 months.

The mean age of patients in the group with a normal FAF appearance was 27.6 years (range, 10–52 years), 16.0 years (range, 11–29 years) in the group with an increased FAF pattern, and 29.3 years (range, 11–49 years) in the group with a reduced FAF pattern. There was no statistically significant difference in the ages among the three FAF pattern groups (Kruskal Wallis test; $P < 0.05$). In one of the two patients in whom we detected evidence of progressive change on SD-OCT

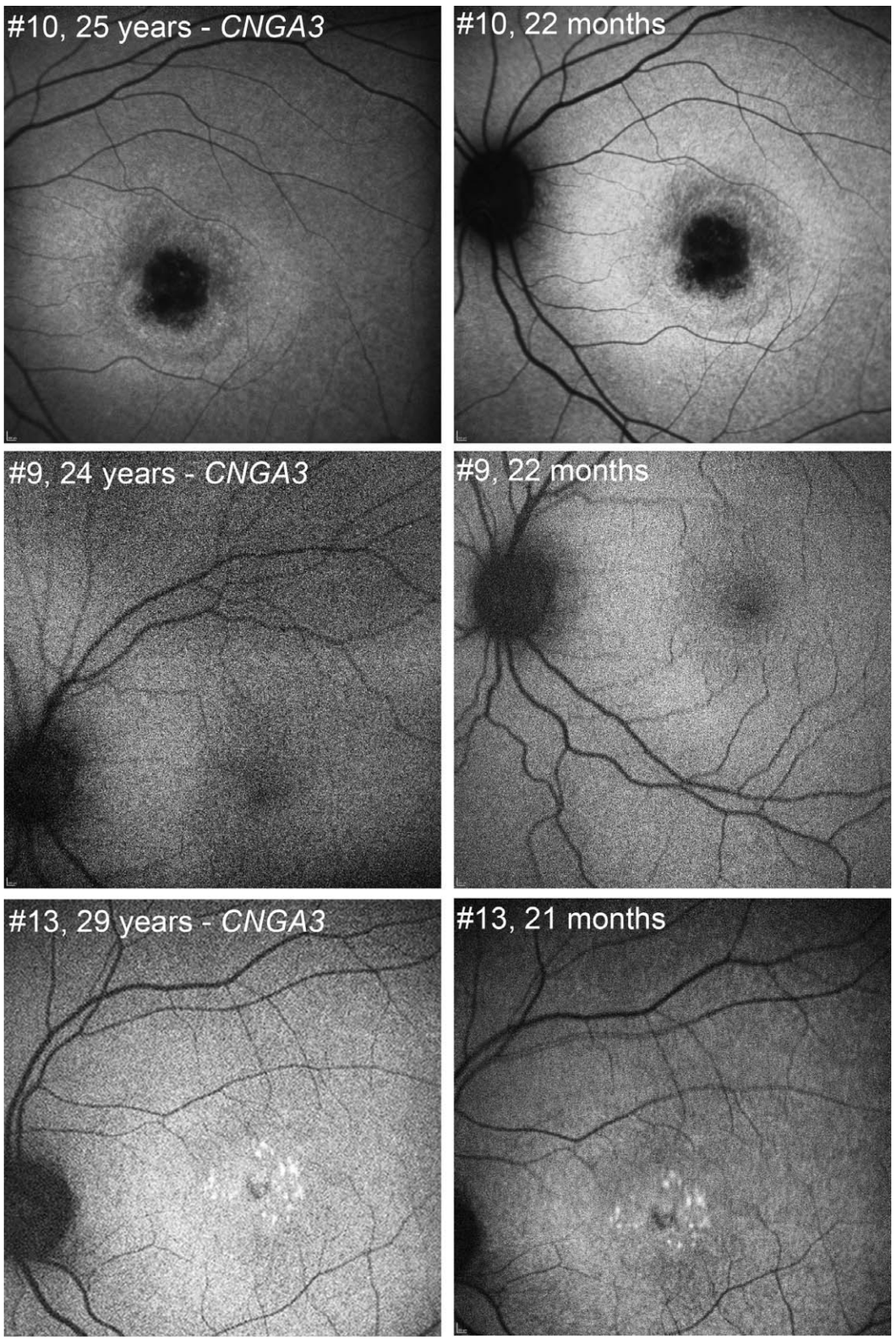

Figure 4. Longitudinal FAF in achromatopsia, demonstrating the three patterns observed (patient number, genotype, and age at baseline acquisition indicated at *left*; patient number and follow-up interval in months indicated at *right*). *Top*: Pattern 1: reduced FAF signal centrally with a well-demarcated border. *Middle*: Pattern 2: normal FAF appearance. *Bottom*: Pattern 3: a central increase in FAF. These patterns were not statistically significantly age dependent. All of the three above patients harbor *CNGA3* disease-causing alleles and are of a similar age, which serves to highlight both the wide phenotypic variation seen in achromatopsia even within the same genotype, and also the lack of strict age-dependency.

Investigative Ophthalmology & Visual Science

(patient 31), there was only a minimal increase in the area of reduced FAF of +0.01 mm^2 over a follow-up time of 20 months; the other patient who progressed on SD-OCT (patient 2) had a normal FAF pattern at both time points.

We observed a statistically significant correlation between more disordered SD-OCT structure (category 1 to 5) and a more abnormal FAF pattern (graded from normal through central increased FAF to central decreased FAF) (Spearman $r = 0.55$; $P = 0.002$).

Genotype–Phenotype Correlation

Of the two patients who progressed on qualitative SD-OCT assessment, one had disease-causing variants in *CNGA3*, and the other in *CNGB3*, suggesting no significant association of progression in *CNGA3* versus *CNGB3*. This would also be in agreement with our previous findings that there was no association between severity of SD-OCT phenotype or presence of foveal hypoplasia, and genotype.[19] However, with only two patients appearing to show progression on SD-OCT, the numbers of progressors by genotype are too small to be anything other than suggestive.

When we analyzed the *CNGA3* and *CNGB3* groups separately, we again did not find any statistically significant difference between the baseline and follow-up measures in BCVA (Wilcoxon matched-pairs test; *CNGA3* $P = 0.75$; *CNGB3* $P = 0.72$), contrast sensitivity (*CNGA3* $P = 0.06$; *CNGB3* $P = 0.11$), MP mean sensitivity (*CNGA3* $P = 0.33$; *CNGB3* $P = 1.0$) or MP mean BCEA (*CNGA3* $P = 1.0$; *CNGB3* $P = 0.41$). There was also no statistically significant difference between the *CNGA3* and *CNGB3* groups in the change in FTRT or ONL thickness (FTRT: Mann-Whitney U test; $P = 0.33$; ONL thickness: unpaired t-test; $P = 0.58$).

In the case of the *CNGA3* and *CNGB3* patients, there was no significant association between the numbers of patients exhibiting each of the three observed FAF patterns and their genotype (χ^2 test; $P = 0.40$).

Discussion

This study is, to the best of our knowledge (PubMed search June 2, 2014; keywords: achromatopsia, rod monochromatism), the largest prospective longitudinal study of ACHM with the longest mean follow-up time of 19.5 months, and sufficient patient numbers for statistical analysis looking for change over time.

Our cohort did not show any evidence of a statistically significant change over time in BCVA, contrast sensitivity, or MP measures of retinal sensitivity and fixation stability, either as whole, or as separate *CNGA3* and *CNGB3* genotype subgroups. Only 2 (5%) of 37 patients followed up longitudinally demonstrated evidence of progressive outer retinal changes according to independently graded qualitative SD-OCT analysis over the follow-up period. Thirty-five patients (95%) demonstrated no qualitative changes on their SD-OCT images between baseline and follow-up assessment. This agrees with our longitudinal quantitative assessment of both TRFT and ONL thickness, both of which showed no statistically significant change in the cohort over the time course of this study. Neither of the two patients (2 and 31) who had a qualitative change in SD-OCT had any significant deterioration over time in their BCVA, contrast sensitivity, MP mean sensitivity, or MP mean BCEA. It has been shown in other inherited retinal conditions that SD-OCT changes may precede deterioration of clinical assessment parameters, such as BCVA[32] and FAF,[33] and so despite a failure to demonstrate deterioration in other clinical measures used in this study, the SD-OCT changes in these two patients likely represent real change. Serial assessment using other sensitive retinal imaging techniques, such as AOSLO, may shed further light on the earliest indicators of any progression in ACHM.

We saw no patients with an ONL or central macular thickness (CMT) thinning of more than 10 μm, which contrasts with Thomas et al.,[20] who report that the five pediatric patients in their study (aged <10 years at first visit) showed SD-OCT evidence of thinning of both CMT and ONL over a mean follow-up time of 13 months. Three of these five children appear to have had an ONL thinning of more than 10 μm, although the numerical values are not stated. The three adults in their study (aged >40 years) showed only minimal variation in these parameters over a mean follow-up of 20 months, in keeping with our study. However, in at least two of the children, the evidence for progression was not unequivocal. Thomas et al.[20] described how patients 1 and 2 had developed an outer retinal hyperreflective zone, which they interpreted as an indication of progression. It should be noted, however, that the same two patients had a generalized increase in reflectivity of several other layers in their respective follow-up OCT images, including the nerve fiber layer and ganglion cell layer, and so the possibility that this apparent increase in outer retinal reflectivity over time may be artifactual remains. Furthermore, they were unable to perform any statistical analyses due to their small sample size. The reason for the difference in our respective findings regarding the evidence for progressive thinning of the ONL and/or CMT may be related to the fact that we had only three children aged 10 years or younger at first visit. However, our cohort did contain a total of eight children aged 12 years or younger at first visit, and the much larger number of patients in our cohort and the consequent ability to carry out a statistical analysis would lend further support to our findings. We also observed no statistically significant change in the diameter of the HRZ in the nine patients in our study who had this finding at both time point assessments.

Fundus Autofluorescence

Our findings of three distinct FAF patterns is in broad agreement with those of Fahim et al.[24] We also found a very small but statistically significant increase in the area of reduced FAF over time among patients who displayed that pattern, indicating that serial FAF may play a role in assessing change in ACHM. There was no statistically significant difference between ages in the three FAF patterns. However, no patients changed their FAF pattern during the time-course of this study, and the rate of increase in the size of reduced FAF was very slow (median 0.02 mm^2/y); by comparison, FAF atrophy rates in AMD are several orders of magnitude greater, in the realm of several mm^2 per year.[29] In addition, there were three patients aged 13 years or younger in the group that had a normal FAF pattern, and one young patent (11 years old) who had a reduced FAF pattern. This again is in keeping with a highly variable disease, where age and genotype are insufficient predictors of phenotype (Fig. 4). However, caution needs to be exercised in overinterpreting these data and no definitive conclusions can be reached without larger cohorts.

We also observed a moderately strong correlation between degree of foveal SD-OCT structural disorganization and degree of FAF abnormality. Fundus autofluorescence intensity may plausibly progress in sequence, from normal signal through increased FAF signal to subsequent FAF signal reduction. It is also possible that the five SD-OCT categories represent a sequence in the severity of foveal outer retinal structure disorganization (from a continuous ISe to outer retinal atrophy), thereby suggesting that the observed correlation of SD-OCT outer retinal architecture to FAF pattern may be of prognostic value, in addition to potentially acting as a further

Investigative Ophthalmology & Visual Science

possible metric in treatment trials. Longer follow-up with larger molecularly confirmed cohorts, combined with more quantitative assessment of FAF, are required to establish whether SD-OCT structural abnormality precedes or follows FAF abnormalities in ACHM.

The diagnostic and prognostic relevance of FAF in ACHM has yet to be established. Robson et al.[34] demonstrated that increased FAF in cone or cone-rod dystrophy is associated with reduced rod and cone sensitivity, with scotopic sensitivity reductions being milder than photopic losses. In contrast, in AMD, increased FAF may be more indicative of rod as opposed to cone dysfunction.[35] We found that the MP mean retinal sensitivity (averaged between the two assessments at each time point) was significantly higher in the increased FAF group (median 18.71 dB) compared with the decreased FAF group (median 17.33 dB) (Mann-Whitney U test; $P = 0.008$), but did not find any statistically significant difference in retinal sensitivity between normal FAF and increased FAF groups (Mann-Whitney U test; $P = 0.19$). In terms of monitoring for progressive change, it would seem that this measure, like the others we have investigated, would need to be assessed over a greater time span, given the likely slow rate of change. This factor, along with the significant degree of patient variability observed, also highlights the need to consider patients on an individual basis in terms of potential suitability for intervention. The use of further quantitative FAF analyses[24,35,36] may increase the sensitivity of FAF assessment in ACHM, but it is still likely that any progression by this measure will occur at a very slow rate in a subset of patients.

Age-Dependency of Progression

In their retrospective study, Thiadens et al.[37] reported that, over a mean follow-up of 15 years, 12% of the ACHM patients they reviewed had a deterioration in BCVA; in contrast with other cross-sectional studies that have not found an age-dependent deterioration in BCVA.[16,17,19] In their longitudinal study of eight patients, Thomas et al.[20] also showed no evidence of a decrease in BCVA over the mean follow-up of 18 months. Khan et al.[3] also reported that 6 to 12 years had elapsed between their detecting and subsequently failing to detect photopic ERG response in two affected adult *CNGB3* individuals. Given the aforementioned time spans, it is likely that any progression in this condition is very slow and possibly subtle; it may be that to see clear evidence of progression in more patients, longitudinal studies of a much longer time course that may extend into many years or even decades would be required.

There is also significant phenotypic variation among individuals in terms of the existence and time course of any such progression. This phenotypic variability is illustrated in the findings of OCT studies[16,19,38–40] and AOSLO studies.[18,41,42] Such variation may confound attempts to look for progression en bloc in what is likely to be a more heterogeneous condition than previously thought. Our data suggest that each individual patient's phenotype, and the significance and time course of any progression, does not correlate with genotype and is highly variable among individuals. Probing this more deeply may require more detailed longitudinal cellular phenotyping with ultrastructural assessments such as AOSLO, potentially in concert with AO-guided psychophysical assessments. The need for such deep-phenotyping has clear implications for the selection and monitoring of patients for anticipated therapeutic interventions. For most of the retinal parameters measured, our initial cross-sectional study did not find any association with *CNGA3* or *CNGB3* genotype.[19] However, we did observe that retinal sensitivity was significantly higher in the *CNGB3* group. This longitudinal study did not identify any measured parameters that worsened significantly between time points when each genotype group was analyzed alone.

The longitudinal findings herein broadly agree with our initial cross-sectional study that age and genotype are not necessarily the critical factors in selecting patients for gene therapy. The vast majority of parameters assessed in this study did not change over time, and those that did, either did so very slowly, or in a very small proportion of patients. This supports the view that the potential treatment window for gene therapy may not only be wider in terms of age than has been previously suggested, but that it may remain open for a longer period. Our data also lend support to the view that ACHM is heterogeneous, and that factors other than age and genotype are likely to influence the phenotype. Such factors may have an as-of-yet unknown influence on any planned therapeutic interventions.

Acknowledgments

The authors thank Vincent Rocco and Monica Clemo for their work on SD-OCT image acquisition, and all the patients and their families for their time and cooperation in taking part in this study.

Supported by grants from the National Institute for Health Research Biomedical Research Centre at Moorfields Eye Hospital NHS Foundation Trust and UCL Institute of Ophthalmology, Fight for Sight, Moorfields Eye Hospital Special Trustees, The Wellcome Trust (099173/Z/12/Z), Retinitis Pigmentosa Fighting Blindness, and the Foundation Fighting Blindness (USA). Also supported by a Foundation Fighting Blindness Career Development Award (MM), a Burroughs Wellcome Fund Career Award at the Scientific interface (AD), and a Career Development Award from Research to Prevent Blindness (AD). JWB is a research professor with National Institute for Health Research. Medical College of Wisconsin supported by National Institutes of Health grants R01EY017607, P30EY001931, and C06RR016511; Foundation Fighting Blindness; and an unrestricted departmental grant from Research to Prevent Blindness. The authors alone are responsible for the content and writing of the paper.

Disclosure: **J. Aboshiha**, None; **A.M. Dubis**, None; **J. Cowing**, None; **R.T.A. Fahy**, None; **V. Sundaram**, None; **J.W. Bainbridge**, None; **R.R. Ali**, None; **A. Dubra**, None; **M. Nardini**, None; **A.R. Webster**, None; **A.T. Moore**, None; **G. Rubin**, None; **J. Carroll**, None; **M. Michaelides**, None

References

1. Michaelides M, Hunt DM, Moore AT. The cone dysfunction syndromes. *Br J Ophthalmol*. 2004;88:291–297.
2. Andréasson S, Tornqvist K. Electroretinograms in patients with achromatopsia. *Acta Ophthalmol (Copenh)*. 1991;69:711–716.
3. Khan NW, Wissinger B, Kohl S, Sieving PA. CNGB3 achromatopsia with progressive loss of residual cone function and impaired rod-mediated function. *Invest Ophthalmol Vis Sci*. 2007;48:3864–3871.
4. Hess R, Nordby K. Spatial and temporal limits of vision in the achromat. *J Physiol*. 1986;371:365–385.
5. Wissinger B, Jägle H, Kohl S, et al. Human rod monochromacy: linkage analysis and mapping of a cone photoreceptor expressed candidate gene on chromosome 2q11. *Genomics*. 1998;51:325–331.
6. Sundin OH, Yang J-M, Li Y, et al. Genetic basis of total colour blindness among the Pingelapese islanders. *Nat Genet*. 2000; 25:289–293.
7. Johnson S. Achromatopsia caused by novel mutations in both CNGA3 and CNGB3. *J Med Genet*. 2004;41:e20.
8. Kohl S, Baumann B, Rosenberg T, et al. Mutations in the cone photoreceptor G-Protein α-subunit gene GNAT2 in patients with achromatopsia. *Am J Hum Genet*. 2002;71:422–425.

9. Chang B, Grau T, Dangel S, et al. A homologous genetic basis of the murine cpfl1 mutant and human achromatopsia linked to mutations in the PDE6C gene. *Proc Natl Acad Sci U S A*. 2009; 106:19581–19586.
10. Kohl S, Coppieters F, Meire F, et al. A nonsense mutation in PDE6H causes autosomal-recessive incomplete achromatopsia. *Am J Hum Genet*. 2012;91:527–532.
11. Alexander JJ, Umino Y, Everhart D, et al. Restoration of cone vision in a mouse model of achromatopsia. *Nat Med*. 2007;13: 685–687.
12. Komaromy AM, Alexander JJ, Rowlan JS, et al. Gene therapy rescues cone function in congenital achromatopsia. *Hum Mol Genet*. 2010;19:2581–2593.
13. Michalakis S, Mühlfriedel R, Tanimoto N, et al. Restoration of cone vision in the CNGA3$^{-/-}$ mouse model of congenital complete lack of cone photoreceptor function. *Mol Ther*. 2010;18:2057–2063.
14. Carvalho LS, Xu J, Pearson RA, et al. Long-term and age-dependent restoration of visual function in a mouse model of CNGB3-associated achromatopsia following gene therapy. *Hum Mol Genet*. 2011;20:3161–3175.
15. Wen R, Tao W, Li Y, Sieving PA. CNTF and retina. *Prog Retin Eye Res*. 2012;31:136–151.
16. Thiadens AA, Somervuo V, van den Born LI, et al. Progressive loss of cones in achromatopsia: an imaging study using spectral-domain optical coherence tomography. *Invest Ophthalmol Vis Sci*. 2010;51:5952–5957.
17. Thomas MG, Kumar A, Kohl S, Proudlock FA, Gottlob I. High-resolution in vivo imaging in achromatopsia. *Ophthalmology*. 2011;118:882–887.
18. Genead MA, Fishman GA, Rha J, et al. Photoreceptor structure and function in patients with congenital achromatopsia. *Invest Ophthalmol Vis Sci*. 2011;52:7298–7308.
19. Sundaram V, Wilde C, Aboshiha J, et al. Retinal structure and function in achromatopsia: implications for gene therapy. *Ophthalmology*. 2014;121:234–245.
20. Thomas MG, McLean RJ, Kohl S, Sheth V, Gottlob I. Early signs of longitudinal progressive cone photoreceptor degeneration in achromatopsia. *Br J Ophthalmol*. 2012;96:1232–1236.
21. Delori FC, Dorey CK, Staurenghi G, Arend O, Goger DG, Weiter JJ. In vivo fluorescence of the ocular fundus exhibits retinal pigment epithelium lipofuscin characteristics. *Invest Ophthalmol Vis Sci*. 1995;36:718–729.
22. Schmitz-Valckenberg S, Holz FG, Bird AC, Spaide RF. Fundus autofluorescence imaging: review and perspectives. *Retina*. 2008;28:385–409.
23. Michaelides M, Aligianis I, Holder G, et al. Cone dystrophy phenotype associated with a frameshift mutation (M280fsX291) in the α-subunit of cone specific transducin (GNAT2). *Br J Ophthalmol*. 2003;87:1317–1320.
24. Fahim AT, Khan NW, Zahid S, et al. Diagnostic fundus autofluorescence patterns in achromatopsia. *Am J Ophthalmol*. 2013;156:1211–1219.e2.
25. Greenberg JP, Sherman J, Zweifel SA, et al. Spectral-domain optical coherence tomography staging and autofluorescence imaging in achromatopsia. *JAMA Ophthalmol*. 2014;132:437–445.
26. Menke MN, Dabov S, Knecht P, Sturm V. Reproducibility of retinal thickness measurements in healthy subjects using Spectralis optical coherence tomography. *Am J Ophthalmol*. 2009;147:467–472.
27. Maheshwary AS, Oster SF, Yuson RMS, Cheng L, Mojana F, Freeman WR. The association between percent disruption of the photoreceptor inner segment–outer segment junction and visual acuity in diabetic macular edema. *Am J Ophthalmol*. 2010;150:63–67.e1.
28. Oster SF, Mojana F, Brar M, Yuson RM, Cheng L, Freeman WR. Disruption of the photoreceptor inner segment/outer segment layer on spectral domain-optical coherence tomography is a predictor of poor visual acuity in patients with epiretinal membranes. *Retina*. 2010;30:713–718.
29. Holz FG, Bindewald-Wittich A, Fleckenstein M, Dreyhaupt J, Scholl HP, Schmitz-Valckenberg S. Progression of geographic atrophy and impact of fundus autofluorescence patterns in age-related macular degeneration. *Am J Ophthalmol*. 2007; 143:463–472.e2.
30. Dreyhaupt J, Mansmann U, Pritsch M, Dolar-Szczasny J, Bindewald A, Holz F. Modelling the natural history of geographic atrophy in patients with age-related macular degeneration. *Ophthalmic Epidemiol*. 2005;12:353–362.
31. Crossland MD, Dunbar HM, Rubin GS. Fixation stability measurement using the MP1 microperimeter. *Retina*. 2009; 29:651–656.
32. Park SJ, Woo SJ, Park KH, Hwang J-M, Chung H. Morphologic photoreceptor abnormality in occult macular dystrophy on spectral-domain optical coherence tomography. *Invest Ophthalmol Vis Sci*. 2010;51:3673–3679.
33. Gomes NL, Greenstein VC, Carlson JN, et al. A comparison of fundus autofluorescence and retinal structure in patients with Stargardt disease. *Invest Ophthalmol Vis Sci*. 2009;50:3953–3959.
34. Robson AG, Michaelides M, Luong V, et al. Functional correlates of fundus autofluorescence abnormalities in patients with RPGR or RIMS1 mutations causing cone or cone-rod dystrophy. *Br J Ophthalmol*. 2008;92:95–102.
35. Scholl HP, Bellmann C, Dandekar SS, Bird AC, Fitzke FW. Photopic and scotopic fine matrix mapping of retinal areas of increased fundus autofluorescence in patients with age-related maculopathy. *Invest Ophthalmol Vis Sci*. 2004;45:574–583.
36. Smith RT, Koniarek JP, Chan J, Nagasaki T, Sparrow JR, Langton K. Autofluorescence characteristics of normal foveas and reconstruction of foveal autofluorescence from limited data subsets. *Invest Ophthalmol Vis Sci*. 2005;46:2940–2946.
37. Thiadens AA, Slingerland NW, Roosing S, et al. Genetic etiology and clinical consequences of complete and incomplete achromatopsia. *Ophthalmology*. 2009;116:1984–1989. e1.
38. Varsányi B, Somfai GM, Lesch B, Vámos R, Farkas Á. Optical coherence tomography of the macula in congenital achromatopsia. *Invest Ophthalmol Vis Sci*. 2007;48:2249–2253.
39. Barthelmes D, Sutter FK, Kurz-Levin MM, et al. Quantitative analysis of OCT characteristics in patients with achromatopsia and blue-cone monochromatism. *Invest Ophthalmol Vis Sci*. 2006;47:1161–1166.
40. Nishiguchi KM, Sandberg MA, Gorji N, Berson EL, Dryja TP. Cone cGMP-gated channel mutations and clinical findings in patients with achromatopsia, macular degeneration, and other hereditary cone diseases. *Hum Mutat*. 2005;25:248–258.
41. Merino D, Duncan JL, Tiruveedhula P, Roorda A. Observation of cone and rod photoreceptors in normal subjects and patients using a new generation adaptive optics scanning laser ophthalmoscope. *Biomed Opt Express*. 2011;2:2189–2201.
42. Carroll J, Choi SS, Williams DR. In vivo imaging of the photoreceptor mosaic of a rod monochromat. *Vision Res*. 2008;48:2564–2568.

ED: Please verify the accuracy of any edits made to the article summary below.

Serial assessment of achromatopsia using multiple imaging and functional modalities reveals limited and slow rates of

Investigative Ophthalmology & Visual Science

progression, the implications of which are discussed in the context of imminent clinical gene therapy trials.

Investigative Ophthalmology & Visual Science